Available online at www.sciencedirect.com

ScienceDirect

Physics Procedia 83 (2016) 147 – 156

Physics Procedia

9th International Conference on Photonic Technologies - LANE 2016

Processing of polyamide electrospun nanofibers with picosecond uv-laser irradiation

Marco Götze[a,*], Olaf Krimig[a], Tobias Kürbitz[b], Sven Henning[c], Andreas Heilmann[b,c], Georg Hillrichs[a]

[a] University of Applied Sciences Merseburg, Eberhard-Leibnitz-Str.2, 06217 Merseburg, Germany
[b] University of Applied Sciences Anhalt, Bernburger Str. 55, 06266 Köthen, Germany
[c] Fraunhofer Institute for Microstructure of Materials and Systems IMWS, Walter-Hülse-Str.1, 06120 Halle(Saale), Germany

Abstract

To optimize the cell colonization on electrospun polyamide nanofibers, the fiber scaffolds were processed with picosecond uv-laser irradiation. The ablation thresholds were determined in dry, wet and immersed condition. The morphology of the ablated areas was evaluated by confocal and scanning electron microscopy. It was found that the ablation thresholds of the nanofiber tissues are lower as for polyamide bulk material. While on bulk samples the ablation spot sizes are close to the focal diameter, on the fiber samples the ablation spots are more extended. Light scattering in the fiber tissue has to be taken into account. The results show that with exact setting of the laser parameters it is possible to reduce the heat-affected zone to a few micrometer. In addition, changing of the nanofiber tissue wettability by laser radiation was investigated.

Peer-review under responsibility of the Bayerisches Laserzentrum GmbH

Keywords: Picosecond laser; laser ablation; polyamide nanofibers; electrospinning; ablation threshold; uv-laser

1. Introduction

In the field of tissue engineering materials and systems are developed to support or substitute diseased tissues or organs (Wintermantel and Ha 2009). Cell carrier systems of electrospun polyamide (PA) nanofibers have great potential, since they offer a favorable ratio of surface area to volume and high mechanical stability. Several studies on the cytotoxicity also confirm the potential use of polyamide for short time implantates (Wintermantel and Ha

* Corresponding author. Tel.: +49-3461-46-2195 ; fax: +49-3461-46-2017 .
E-mail address: marco.goetze@hs-merseburg.de

Peer-review under responsibility of the Bayerisches Laserzentrum GmbH
doi:10.1016/j.phpro.2016.08.028

2009). Studies on different cell carrier systems of electrospun polymers have already shown that the growth and proliferation of settled cells are controlled by direct modification of the surface of the support system (Lim et al. 2011). The surface structure and chemistry of these tissue replacement systems have significant influence on the adhesion, development and functionality of cells (Lim et al. 2011).

Laser systems with ultra short pulses can be used for modification and processing of electrospun mats (Choi et al. 2007; He et al. 2011; Lee et al. 2011; Jenness et al. 2012; Kim et al. 2014; Adomavičiūtė et al. 2015). In contrast to laser machining with pulse durations in the nanosecond range ultrafast processing with femtosecond-laser pulses often takes place without substantial heat transfer to the surrounding material (Wu et al. 2011). Today ultraviolet (uv) picosecond (ps) lasers are reliable and comparably compact systems for industrial micro material processing. So in this work the use of uv-laser pulses with pulse durations of several ps where investigated as an possible alternative for femtosecond (fs) laser pulses for processing of polyamide 6.6 bulk material and nanofiber tissues. To selectively modify the surfaces of the nanofiber tissues for the control of cell growth accurate knowledge of ablation thresholds and laser generated changes in the topography of the materials used is necessary (Baudach et al. 2000; Gedvilas and Raciukaitis 2005).

2. Materials and Methods

2.1. Electrospun polyamide nanofiber scaffolds

Polyamide 6.6 (Sigma Aaldrich) was dissolved in a blend of 50% acetic acid (Carl Roth) and 50% formic acid (Carl Roth) to a concentration of 15% (w/v). The commercial electrospinning device “Nanospider” (Elmarco) was used for the electrospinning process. The process was carried out at 80 kV with a working distance of the electrodes at 240 mm. The temperature was kept at 22°C and the relative humidity was about 30%.

2.2. Picosecond laser ablation

The experimental setup was based on a Nd:YAG laser system (Coherent Talisker 355-4) with the following parameters: wavelength $\lambda = 355$ nm, pulse duration $\tau_p = 15$ ps, repetition rate f_{Rep} up to 200 kHz, maximum output pulse energy $Q = 26$ µJ and a beam quality factor $M^2 < 1.3$. The laser radiation was focused onto the surface of the sample by an f-theta lens with a focal length of 103.2 mm giving a spot diameter of 13.6 µm. The spot diameter was deterimined in previous experiments with different bulk materials using the D^2-model described in chapter 3.1. A galvoscanning system (Nutfield Razor Head 10) guided the laser beam across the sample and was controlled by the software SAMLight. In addition, the sample could be moved using a computer-controlled x-y-z stage.

2.3. Microscopy

The processed samples were evaluated with various microscopic techniques. Scanning electron microscope (SEM) images were taken with a Phenom (LOT). The samples were coated with thin layers of carbon or platinum. For optical microscopy an Olympus microscope (BX 60) with a camera (SC 50) was used.

2.4. Contact angle / Wettability

To quantify the surface wettability, the water contact angle of sessile drops was measured at room temperature and under ambient air conditions using a drop shape analyzer (DSA25E, Krüss). Sessile drops were comprised of 2µl deionized water and were released onto the substrate surface through a (1 ml, 0.5 mm diameter) syringe and observed by a camera.

3. Results and Discussion

3.1. Ablation threshold

To determine the ablation threshold F_{th} of the polyamide nanofibers and of the bulk material the sample surface was processed with different numbers of laser pulses focused on one point of the sample. To evaluate the results the D²-model by Liu (1982) was used, which predicts a correlation between the square of the measured ablation spot D and the laser fluence F_0 (Eq. 1).

$$D^2 = 2{w_0}^2 \ln\left(\frac{F_0}{F_{th}}\right) \tag{1}$$

With the pulse energy Q and the focal radius w_0 of the Gaussian laser beam on the sample surface the average laser fluence F_0 was calculated according to Eq. 2.

$$F_0 = \frac{Q}{\pi {w_0}^2} \tag{2}$$

The threshold fluence F_{th} results from the linear correlation of D² and ln (F_0) (Eq. 3), where n is the D²-axis intercept.

$$F_{th} = \frac{e^{\left(-\frac{n}{2{w_0}^2}\right)}}{\pi {w_0}^2} \tag{3}$$

The model provides realistic threshold fluences for single pulse ablation (Ben-Yakar and Byer 2004). Typical single pulse ablation spots of the nanofiber tissue are shown in Fig. 1. It is evident that the ablation spot size decreases with the fluence. The threshold fluence of polyamide nanofibers at single pulse ablation was derived from the data shown in Fig.2a. From corresponding measurements with 10 and 100 pulses the multi pulse ablation thresholds were determined. With increasing number of pulses the ablation threshold decreases (F_{th} = 0.12 J / cm² at 1 pulse, F_{th} = 0.07 J / cm² at 10 pulses and F_{th} = 0.05 J / cm² at 100 pulses). This behavior is due to an incubation effect, which has already been demonstrated in several studies for other materials (Baudach et al. 2000; Ben-Yakar and Byer 2004). According to Bonse et al. (2002) the material-dependent coefficient ξ (Eq. 4) describes the relationship between single pulse ablation threshold and multi (N) pulse ablation threshold.

$$F_{th}(N) = F_{th}(N = 1)N^{\xi - 1} \tag{4}$$

For materials with ξ = 1 no incubation could be observed. The coefficient ξ was calculated for the polyamide nanofiber ablation (Fig. 2b) with ξ = 0.78 and indicates a small incubation effect. This is similar to Polycarbonate (ξ = 0.74) (Baudach et. al. 2000) and less than for polyamide bulk material (ξ = 0.64).

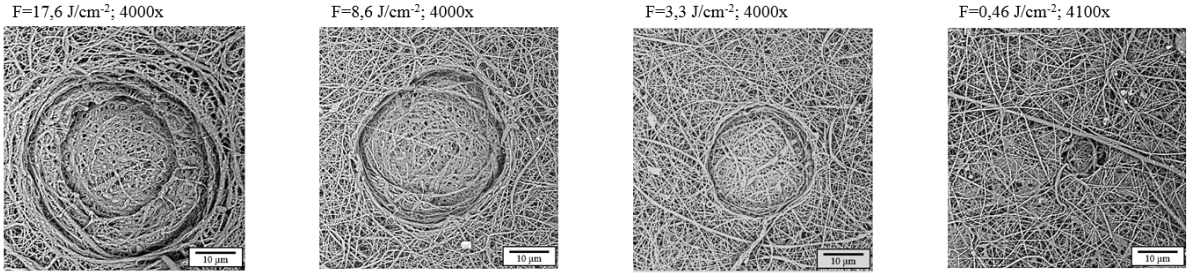

Fig. 1. SEM micrographs of single pulse ablation of polyamide 6.6 nanofiber tissues with different laser fluences.

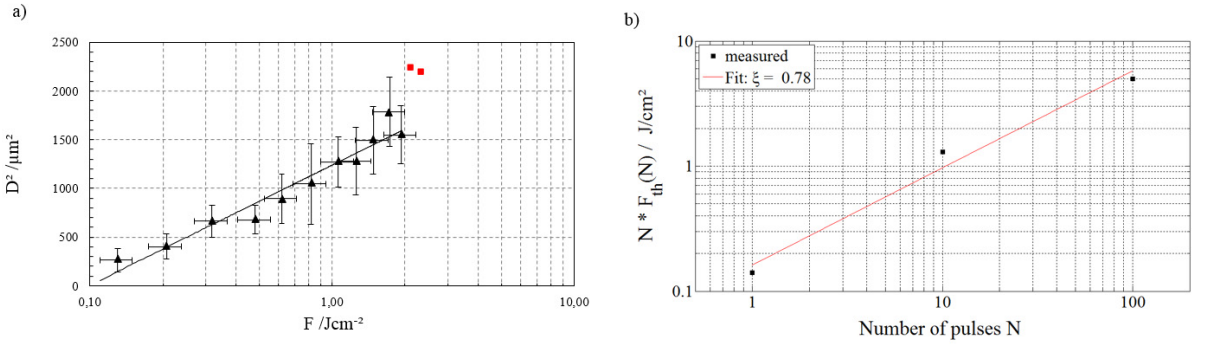

Fig. 2. (a) Single pulse ablation threshold measurements of polyamide nanofibers. D² of the ablated areas is plotted as a function of the laser fluence. The extrapolation of the linear fits to zero provides the ablation threshold F_{th}. The red values indicate the beginning of thermal ablation. (b) Single pulse and multipulse ablation threshold of polyamide nanofibers. The fit indicates the incubation-coefficient ξ.

The ablation thresholds for polyamide 6.6 bulk material were also determined and compared with the nanofiber data (Fig. 3a). The results for 10 pulses are shown in Fig. 3b. For single pulses (Fig. 3a) it was found that the ablation threshold is about 2 J/cm² for bulk PA 6.6 and much higher than the respective threshold of 0.12 J/cm² for the PA nanofiber tissue. For ten pulses the bulk ablation threshold is about 0.07 J/cm².

For ten pulse ablation of the PA nanofiber tissue (Fig. 3b) two different regimes are observed. Above a fluence $F_{th,\,t}$ of about 2.8 J/cm² thermal effects degrade the quality of the laser generated structures. A part of the absorbed laser energy is not used for direct ablation and leads to a temperature increase and melting effects around the laser spot (Engelhardt et al. 2011).

The observation that the bulk ablation thresholds are higher than for the fiber tissue is probably due to the fact that the interaction between the laser and the material is more efficient in the nanofiber network than on the flat bulk surface. Scattered photons can be absorbed by neighboring fibers and cause direct ablation or incubation. In transmission spectroscopic experiments it was found that the extinction of 355 nm light is higher in the fiber material than in the bulk.

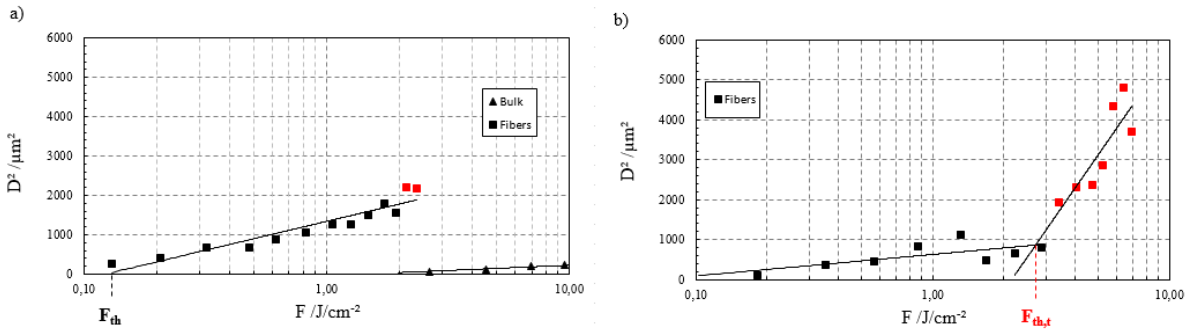

Fig. 3. Results of the ablation threshold determination of a) single pulse ablation of polyamide nanofibers and polyamide bulk material and b) ablation of polyamide nanofibers with 10 pulses. The red values indicate the range of thermal ablation.

3.2. Ablation under wet and immersed condition

For special medical applications it is necessary to process the nanofiber tissues under liquids or under wet conditions. In first studies polyamide nanofiber samples were placed in deionized water for 30 min, then taken out of the water and processed with different numbers of pulses and laser energies at a pulse repetition rate of 100 kHz. Processing of the nanofibers in immersed state was carried out under a defined steady state water level.

The results for single pulse ablation in dry and wet state are shown in Fig.4. The ablation threshold F_{th} of the wet sample is about 0.16 J/cm² and higher than in the dry state. Water absorption and swelling of the fibers have to be taken into account.

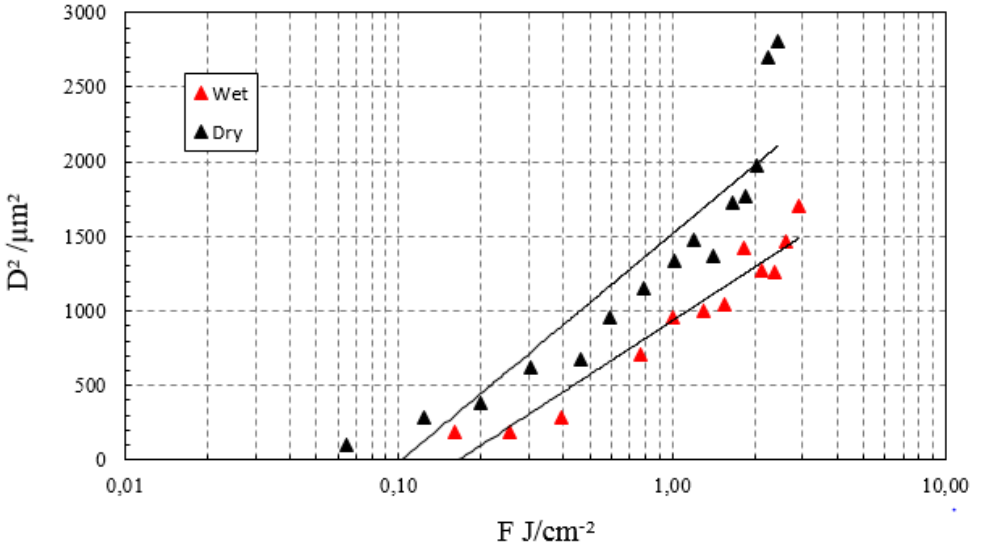

Fig. 4. Single pulse ablation threshold measurements of polyamide nanofibers under dry and wet condition.

The ablation threshold of polyamide nanofibers under immersed condition could only be narrowed phenomenologically. For this squares with an edge length of 50 µm were created by the laser with varying pulse energy in the range of calculated laser focus position. Due to the water column above the sample the focal position of the laser changes and complicates the accurate determination of the single pulse diameter. The contours were generated by about 280 pulses at each position. The threshold fluence could be limited to a range from above 0.4 J/cm² (no ablation) to below 1.3 J/cm².

3.3. Characterization of the ablated areas

3.3.1. Ablation spot size

The investigations of the polyamide nanofiber tissues and the bulk material of polyamide 6.6 have shown clear differences in the diameter of the laser ablated spot (Fig. 5), depending on the number of pulses and pulse energy used.

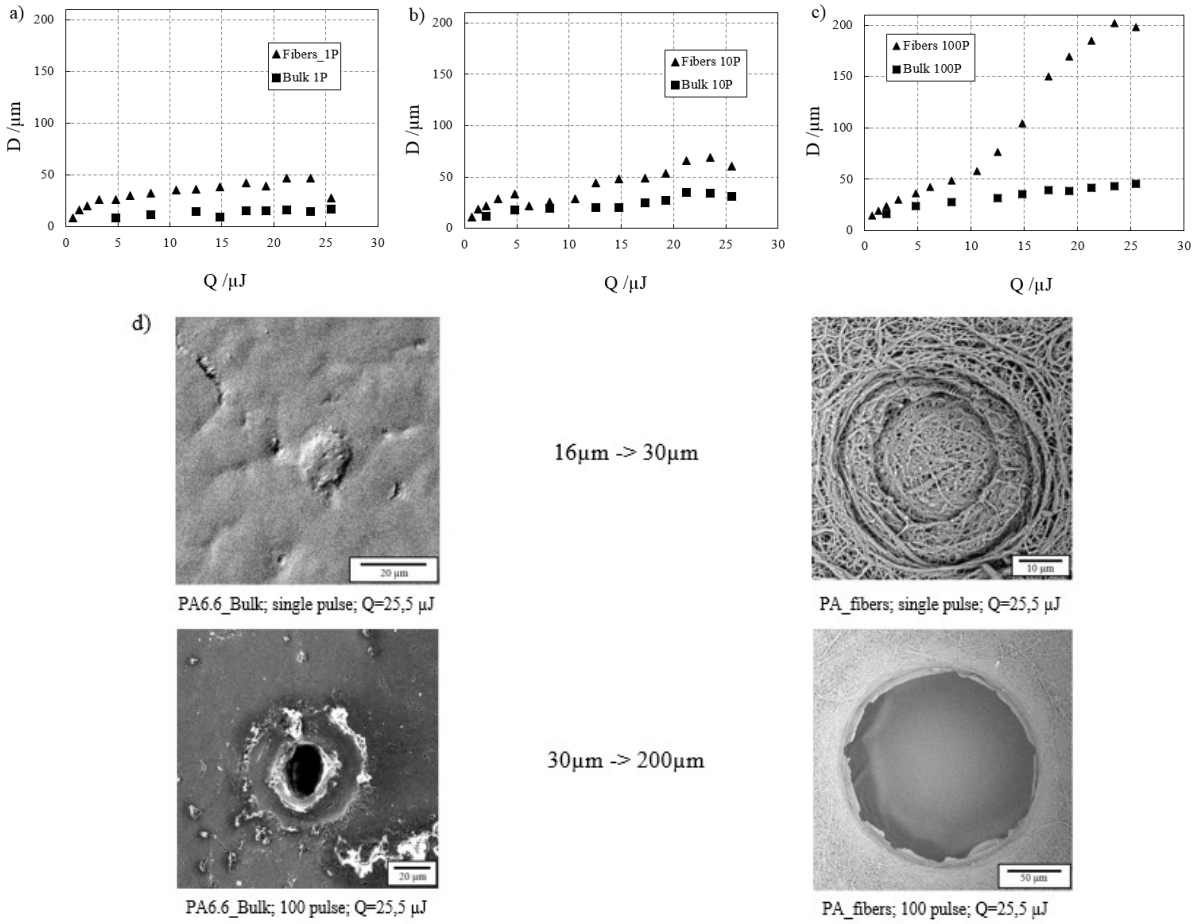

Fig. 5. Differences in the measured diameters in polyamide nanofibers and polyamide bulk material from (a) single pulse ablation (b) 10 pulses and (c) 100 pulses.(d) SEM micrographs of ablated area on polyamide bulk material and polyamide nanofibers. At high pulse counts the measured diameters are considerably larger than for the bulk material.

While the ablated areas of bulk material are in the range of the focal diameter of the Gaussian beam the diameter of nanofiber ablation spots are significantly greater (Fig. 5). In Fig. 6 the spot sizes of bulk and nanofiber tissue ablation are compared with the Gaussian beam profile of the laser. For bulk PA no ablation is observed for surface regions where the fluence of the undisturbed Gaussian beam is below the ablation threshold. For the nanofiber tissue ablation is also observed in surface areas where the fluence of the undisturbed beam is smaller than the respective threshold. Light scattering in the fiber sample is a possible reason for significantly greater diameters at the nanofiber ablation. It is also possible that optical radiation from the laser generated plasma leads to a stronger increase of the affected surface (Adomavičiūtė et al. 2015) in the fiber samples than in the bulk samples. However, other materials and longer laser wavelengths were used in these studies of Adomavičiūtė et al. (2015). The thickness of the polyamide nanofibers is in the same order of magnitude as the wavelength of 355 nm, so that Mie-like scattering has to be considered. Differences in the effective density and therefore in the thermal capacity and thermal conductivity between the bulk and the fiber material will influence the extension of the laser affected area and the heat-affected zone.

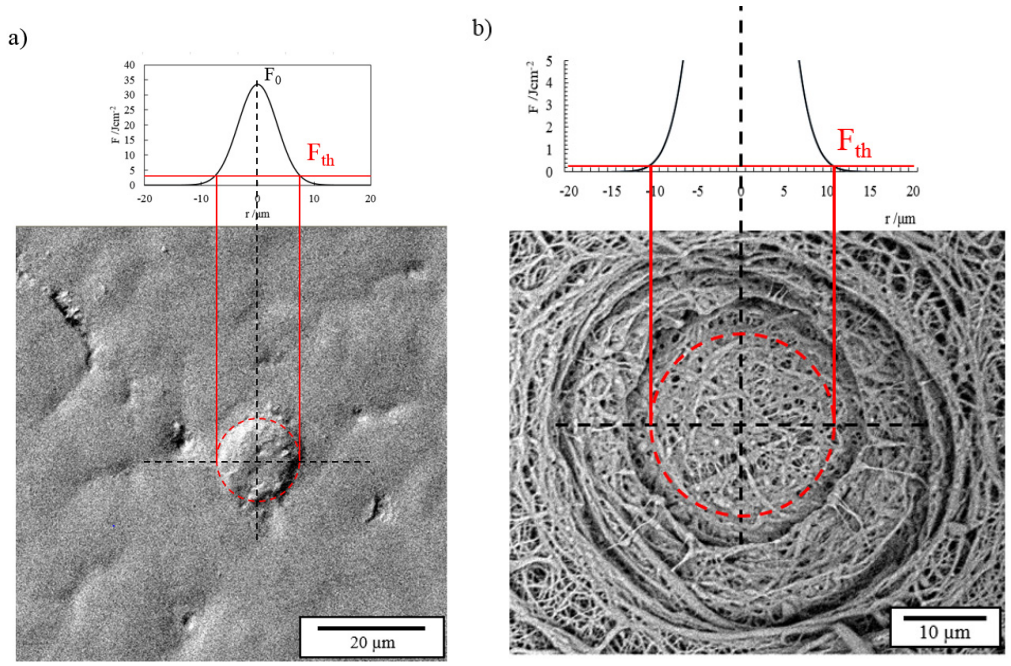

Fig. 6. SEM micrographs of polyamide samples after laser ablation: a) polyamide bulk material (single pulse, F=17, 6 J/cm²), b) polyamide nanofiber tissue (single pulse, F=17, 6 J/cm²).

3.3.2. Heat affected zone

In order to optimize cutting and structuring of nanofiber tissue scaffolds the influence of different laser parameters on line widths, edge quality, heat-affected zone (HAZ) and the pollution of the fibers by ablated particles (debris) was examined. For the first investigation of the heat-affected zones holes with 10 pulses and squares with an edge length of 50 µm were created on the nanofibers samples. The laser fluence was varied. The experiments have shown, that the edge quality is good. Only small HAZ with extensions below about 2 µm around the holes appear. For smaller fluences the HAZ appears to be even smaller (Fig. 7). At high fluences some debris formation was observed.

In Fig. 8 a clean laser cut through a fiber sample obtained with a laser fluence of 2.2 J/cm², a scan speed of 400 mm/s and a repetition rate of 200 kHz is shown.

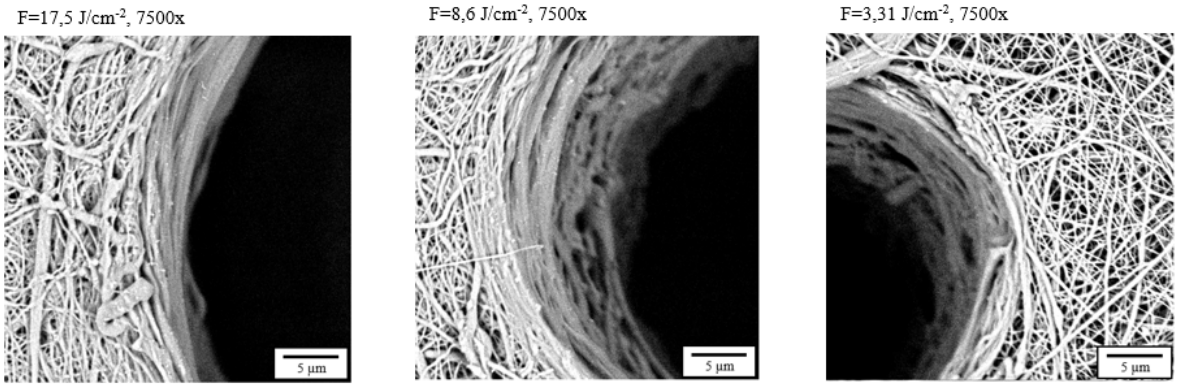

Fig. 7. SEM micrographs of electrospun polyamide nanofibers after uv-laser processing with different laser fluences.

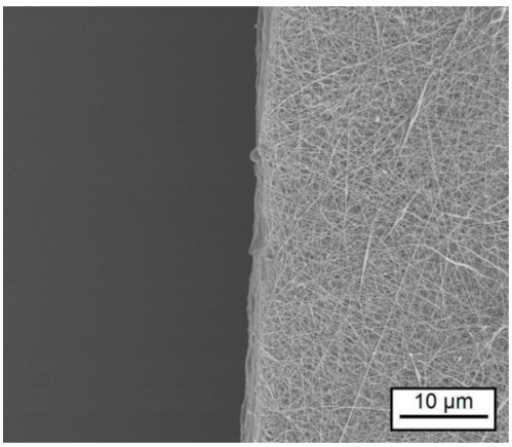

Fig. 8. SEM micrograph of electrospun polyamide nanofibers after uv-laser cutting with 2.2 J/cm².

3.4. Wettability

To investigate the influence of laser processing on the wetting behavior of polyamide bulk material and polyamide nanofiber tissues, which could affect the colonization behavior of cells (Lim et al. 2011), square areas of 10x10 mm were ablated. The ablation was carried out with cross hatch scan pattern with a line spacing of 14 µm, which corresponds to the spot diameter of the laser beam on the sample. The scan speed was 1400 mm/s with only a small overlap of the individual laser pulses along a line (Fig. 9). The laser fluence was varied between 17.5 J/cm² and 0.07 J/cm². For each sample, the contact angle Θ was measured for 10 seconds with one measurement per second. For reference the contact angles were determined on untreated samples. In Fig. 10 the results of the contact angle measurements of polyamide bulk material are shown. The contact angles of the untreated sample was measured between 17° and 21°.

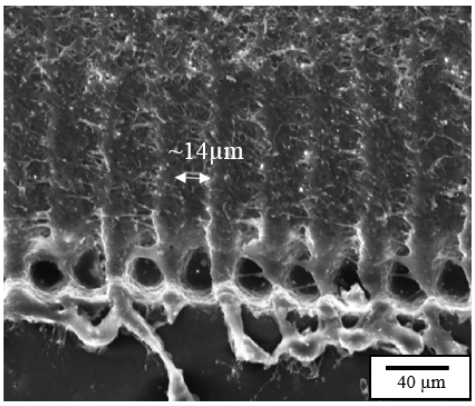

Fig. 9. SEM micrograph of polyamide bulk material after uv-laser processing.

On a processed sample with a laser fluence of 17.5 J/cm² and a significantly higher surface roughness the contact angle is about 25° and thus only slightly higher than in the reference samples. With decreasing laser fluence the contact angle rises to about 70° at 5.6 J/cm². With a laser fluence near the ablation threshold of 1.4 J/cm² the contact angle decreased to about 20-25°. At 0.07 J/cm², which is below the determined ablation threshold, a contact angle of about 15-20° was measured, which corresponds to the contact angle on untreated reference samples.

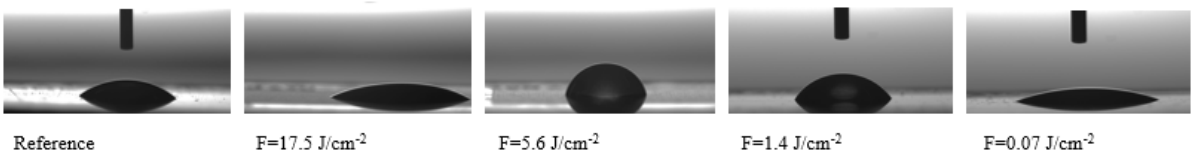

Fig. 10. Images of the contact angle measurements of polyamide bulk material processed with different laser fluences.

So at 5.6 J/cm² the laser generated surface texture leads to a more hydrophobic behavior. Higher and smaller laser fluences generate more hydrophilic surface conditions. In addition to the samples of polyamide bulk material, samples of polyamide nanofiber tissues were also studied with respect to their wetting behavior. Due to the small sample thickness of the nanofibers of about 70-100 µm, a maximum laser fluence of 5.6 J/cm² could not be exceeded, otherwise the samples are completely ablated. In Fig. 11 the results of the contact angle measurements for polyamide-nanofiber tissues are shown.

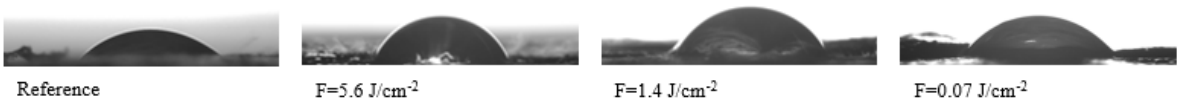

Fig. 11. Images of the contact angle measurements of polyamide nanofiber tissues processed with different laser fluences.

For the untreated reference sample, contact angles in the range of 30-35 ° were measured. With fluences above the ablation threshold between 1.4 J/cm² and 5.6 J/cm² the contact angles were between 40-65°. With a laser fluence below the ablation threshold of 0.07 J/cm², a contact angle of 40° was measured. Due to a soaking behavior of the polyamide nanofibers the contact angle tends to shrink soon after droplet deposition. However, the contact angle leveled out for all measurements in the range of 30°. This corresponds to the determined contact angle of an untreated or non ablated sample. Further studies have to be performed in order to obtain a suitable surface structure

for controlling the wetting behavior without affecting the porous surface structure of the fibers negatively.

4. Conclusions

Ablation thresholds for single pulse processing of electrospun polyamide 6.6 nanofiber tissues in dry and wet state (0.12 and 0.16 J / cm²) were determined for 355 nm laser ablation with picosecond pulses. These levels are well below the ablation threshold of polyamide 6.6 bulk material. In immersed condition the multi pulse ablation thresholds were determined phenomenologically (between 0.4 and 1.3 J/cm²). The results show that water appears to increase the ablation threshold. The ablation of wet or immersed nanofiber tissues will further be investigated with respect to debris formation and heat affected zones.

In addition to a lower threshold fluence, the polyamide nanofibers show a larger ablation area than the bulk material. Light scattering and optical radiation from produced plasma should be taken into account.

Processing of dry nanofiber tissues with uv ps laser radiation is possible with small heat affected zones especially at moderate fluences without strong debris formation. The quality of laser cuts obtained with 355 nm ps laser radiation is very good and comparable to results obtained with femtosecond laser sources at other electrospun nanofiber tissues (Choi et al. 2007; Lim et al. 2011).

First experiments on wetting behavior also show that in certain fluence ranges the contact angle increases both for nanofibers and for bulk material. Further experiments will show whether it will be possible to optimize the wetting behavior of the nanofibers for a possible cell colonization.

Acknowledgements

This work was carried out within the program „Forschung an Fachhochschulen – Förderlinie Ingenieur Nachwuchs“, FKZ: 03FH017IA5 and funded by the Federal Ministry of Education and Research (BMBF).

References

Adomavičiūtė, E., Tamulevicius, T., Simatonis, L., Fataraitė-Urbonienė, E., Stankevicius, T., Tamulevicius, S., 2015. Microstructuring of electrospun mats employing femtosecond laser. Materials Science. 21.

Baudach, S., Bonse, J., Krüger, J., Kautek, W., 2000. Ultrashort pulse laser ablation of polycarbonate and polymethylmethacrylate. Applied Surface Science. 154-155:555–560.

Ben-Yakar, A., Byer, R. L., 2004. Femtosecond laser ablation properties of borosilicate glass. Journal of Applied Physics. 96:5316.

Bonse, J., Baudach, S., Krüger, J., Kautek, W., Lenzner, M., 2002. Femtosecond laser ablation of silicon-modification thresholds and morphology. Applied Physics A. 74(1):19-25.

Choi, H. W., Johnson, J. K., Nam, J., Farson, D. F., Lannutti, J., 2007. Structuring electrospun polycaprolactone nanofiber tissue scaffolds by femtosecond laser ablation. Journal of Laser Applications. 19:225.

Engelhardt, U., Hildenhagen, J., Dickmann, K., 2011. Micromachining using high-power picosecond lasers. Laser Technik Journal. 8:32–35.

Gedvilas, M., Raciukaitis, G., 2005. Processing of Polymers by UV Picosecond Lasers. International Congress on Applications of Lasers & Electro- Optics (ICALEO 2005) Paper #401.

He, L., Chen, J., Farson, D. F., Lannutti, J. J., Rokhlin; S. I., 2011. Wettability modification of electrospun poly(ε-caprolactone) fibers by femtosecond laser irradiation in different gas atmospheres. Applied Surface Science. 257:3547–3553.

Jenness, N. J., Wu, Y., Clark, R. L., 2012. Fabrication of three-dimensional electrospun microstructures using phase modulated femtosecond laser pulses. Materials Letters. 66:360–363.

Kim, M. S., Son, J., Lee, H., Hwang, H., Choi, C. H., Kim, G., 2014. Highly porous 3D nanofibrous scaffolds processed with an electrospinning/laser process. Current Applied Physics. 14:1–7.

Lee, C. H., Lim, Y. C., Farson, D. F., Powell, H. M., Lannutti, J. J., 2011. Vascular wall engineering via femtosecond laser ablation: scaffolds with self-containing smooth muscle cell populations. Annals of biomedical engineering. 39:3031–3041.

Lim, Y. C., Johnson, J., Fei, Z., Wu, Y., Farson, D. F., Lannutti, J. J., Choi, H. W., Lee, L. J., 2011. Micropatterning and characterization of electrospun poly(ε-caprolactone)/gelatin nanofiber tissue scaffolds by femtosecond laser ablation for tissue engineering applications. Biotechnology and bioengineering. 108:116–126.

Liu, J. M. 1982. Simple technique for measurements of pulsed Gaussian-beam spot sizes. Optics Letters. 1981.

Wintermantel, E., Ha, S.-W., 2009. Medizintechnik. Springer Berlin Heidelberg, Berlin, Heidelberg.

Wu, Y., Vorobyev, A., Clark, R. L., Guo, C., 2011. Femtosecond laser machining of electrospun membranes. Applied Surface Science. 257:2432–2435.